

Enhanced Hydrogenation Catalytic Activity of Ruthenium Nanoparticles by Solid-Solution Alloying with Molybdenum

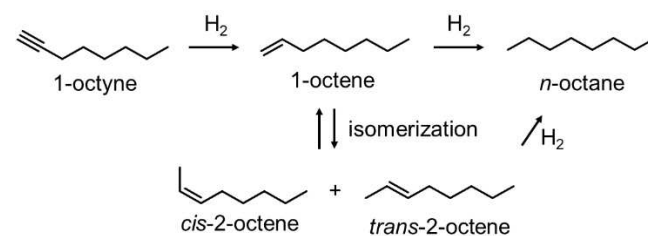
Shinya Okazoe,^[a, b] Lena Staiger,^[a] Mirza Cokoja,^[a] Kohei Kusada,^[b] Tomokazu Yamamoto,^[c] Takaaki Toriyama,^[c] Syo Matsumura,^[c, d] Hiroshi Kitagawa,^[b] and Roland A. Fischer*^[a]

We report the hydrogenation catalytic activity application of molybdenum–ruthenium (MoRu) solid-solution alloy nanoparticles (NPs) as catalysts for the hydrogenation of 1-octene and 1-octyne. The solid-solution structure of MoRu NPs was confirmed through scanning transmission electron microscopy (STEM) coupled with energy-dispersive X-ray spectroscopy (EDX), and powder X-ray diffraction (PXRD) measurement. The hydrogenation catalytic activity of these NPs toward 1-octyne and 1-octene in tetrahydrofuran (THF) was tested. The hydrogenation catalytic activity of Ru was enhanced by alloying with Mo at the atomic level. An electronic modification of Ru by a charge transfer from Mo to Ru, which could induce the change in the adsorption energy of reactants resulting in enhanced catalytic activity, was observed by X-ray photoelectron spectroscopy.

The hydrogenation of unsaturated carbons is an important reaction that is widely used in the chemical industry. From an energy consumption viewpoint, catalysts that can effectively promote the reaction under mild conditions are required. Platinum group metals (PGMs), in particular Pt, Ru, Rh, and Pd, are well known as excellent hydrogenation catalysts for unsaturated hydrocarbons^[1] because these metals can easily dissociate H₂ molecules into H atoms on their surfaces.^[2] Ru has

attracted much attention because of its lower cost and higher hydrogenation catalytic activities toward various substrates.^[3] To tune its catalytic activity, the alloying of Ru with other metals has been studied. Among alloyed structures, solid-solution alloy NPs, where constituent atoms mix at the atomic level, are well investigated because their electronic structures can be easily modified by changing the metal compositions or alloy components. To date, various Ru-based solid-solution alloy NPs, for example, Ru–Pt,^[4] Ru–Pd,^[5] and Ru–Ni,^[6] have been synthesized, and they exhibit higher catalytic activities than Ru. Most of the reported Ru-based solid-solution alloy catalysts are composed of late transition metals. However, Ru-based solid-solution alloy NPs composed of early transition metals such as Mo, W, and Cr are few reported. By contrast, Pt–Cr,^[7] Pd–W,^[8] Pd–Mo,^[9] and Rh–W^[10] solid-solution alloy NPs show higher catalytic activities than monometallic catalysts. Therefore, alloying Ru with early transition metals is challenging and might be effective for enhancing its catalytic activities. In addition, compared with late transition metals, in particular PGMs, early transition metals are much cheaper and more abundant. If the catalytic activity is enhanced by alloying with early transition metals, this could be effective from a cost viewpoint. Recently, we succeeded in the synthesis of solid-solution alloy NPs composed of Mo and Ru, and found their high catalytic activity toward the hydrogen evolution reaction.^[11] In this study, we report on the catalytic activity of MoRu solid-solution alloy NPs for the hydrogenation of 1-octene and 1-octyne as model substrates (Scheme 1).

Ru NPs and MoRu solid-solution alloy NPs were synthesized by thermal decomposition^[11] and denoted as Ru and Mo_{0.2}Ru_{0.8} (see the Supporting Information, SI). The exact atomic ratio of Mo and Ru in MoRu solid-solution alloy NPs was calculated to be 0.19:0.81 by X-ray fluorescence (XRF) spectroscopy. The mean diameters were 6.6 ± 1.1 and 2.7 ± 0.5 nm for Ru and Mo_{0.2}Ru_{0.8} NPs, respectively (SI, Figures S1 and S2 and Table S1). The atomic distribution was determined using scanning trans-



Scheme 1. Reaction scheme of 1-octene and 1-octyne hydrogenations.

[a] S. Okazoe, L. Staiger, Dr. M. Cokoja, Prof. Dr. R. A. Fischer
Department of Chemistry and Catalysis Research Center
Technical University of Munich
Lichtenberg Straße 4, 85748 Garching, Germany
E-mail: roland.fischer@tum.de
www.department.ch.tum.de/amc/home/

[b] S. Okazoe, Dr. K. Kusada, Prof. Dr. H. Kitagawa
Division of Chemistry, Graduate School of Science
Kyoto University
Kitashirakawa-Oiwakecho, Sakyo-ku, 606-8502 Kyoto, Japan

[c] T. Yamamoto, T. Toriyama, Prof. Dr. S. Matsumura
The Ultramicroscopy Research Center
Kyushu University
Motoooka 744, Nishi-ku, 819-0395 Fukuoka, Japan

[d] Prof. Dr. S. Matsumura
Department of Applied Quantum Physics and Nuclear Engineering
Kyushu University
819-0395 Fukuoka, Japan

Supporting information for this article is available on the WWW under
<https://doi.org/10.1002/ejic.202001141>

© 2021 The Authors. European Journal of Inorganic Chemistry published by Wiley-VCH GmbH. This is an open access article under the terms of the Creative Commons Attribution Non-Commercial NoDerivs License, which permits use and distribution in any medium, provided the original work is properly cited, the use is non-commercial and no modifications or adaptations are made.

mission electron microscopy (STEM) and energy dispersive X-ray (EDX) spectroscopy. A high-angle annular dark-field (HAADF)-STEM image, the corresponding Mo-L and Ru-L EDX maps, and an overlay of Mo and Ru maps of $\text{Mo}_{0.2}\text{Ru}_{0.8}$ NPs are shown in Figure 1a–d. The EDX maps clearly show the Mo and Ru atoms to be homogeneously distributed in each NP, indicating a solid-solution alloy structure. In addition, we also confirmed a solid-solution structure through STEM-EDX line analysis (Figure S3). The crystal structure of the synthesized NPs was examined using powder X-ray diffraction (PXRD) (SI, Figure S4), and the patterns were refined by the Le Bail method (SI, Figures S5 and S6). The calculated lattice constants of $\text{Mo}_{0.2}\text{Ru}_{0.8}$ NPs ($a=2.7706 \text{ \AA}$, $c=4.3289 \text{ \AA}$ for a hcp structure, $a=3.8530 \text{ \AA}$ for a fcc structure) were slightly larger than those of Ru NPs ($a=2.7109 \text{ \AA}$, $c=4.2879 \text{ \AA}$ for a hcp structure, $a=3.8202 \text{ \AA}$ for a fcc structure), which indicates alloying Ru with Mo which has a larger atomic radius. These results support the formation of a solid-solution alloy with lattice parameters that are larger than those of Ru, as previously reported.^[11]

These NPs were applied in the catalytic hydrogenation of unsaturated hydrocarbons (1-octene and 1-octyne) (Scheme 1). Hydrogenation tests were performed with 1 mol% NPs toward the substrates in 2.4 mL of tetrahydrofuran (THF). A 0.05 mL substrate and 0.05 mL *n*-dodecane as an internal standard were added to the solutions. Next, H_2 was introduced into the reactor under a pressure of 1 or 3 bar. The concentrations of substrates and products were determined by gas chromatography. The details of the catalytic tests are described in SI. In general, the size of NPs is one of the factors to determine the catalytic activity, and comparable sizes of NPs should be used for a fair comparison. However, we used different sizes of NPs because

the comparable size of NPs could not be prepared by the thermal decomposition.

The time dependence of catalytic conversion of 1-octene at 60°C is presented in Figure 2a. 1-octene was converted to *n*-octane on Ru and $\text{Mo}_{0.2}\text{Ru}_{0.8}$ NPs within 15 min. $\text{Mo}_{0.2}\text{Ru}_{0.8}$ NPs showed a catalytic activity comparable or slightly higher than Ru NPs, and the same tendency was observed at 30°C (Figure 2b). Small amounts of the isomers *cis*-2-octene and *trans*-2-octene were also observed during hydrogenation; the time-dependent concentration of C8 species is shown in Figure S8 and Figure S9. These isomers were also converted to *n*-octane in the end.

We further performed hydrogenation of 1-octyne under 3 bar H_2 at 60°C . The concentrations of 1-octyne, 1-octene, *trans*-2-octene, *cis*-2-octene, and *n*-octane normalized without oligomers are shown in Figure 3a and Figure 3b, and the final concentration of the solution is shown in Table 1. Full conversion of 1-octyne over Ru NPs reached at 60 min, whereas that over $\text{Mo}_{0.2}\text{Ru}_{0.8}$ NPs reached at 45 min. $\text{Mo}_{0.2}\text{Ru}_{0.8}$ showed a much higher catalytic activity for 1-octyne than Ru, which demonstrated that alloying Ru with early transition metal is also effective in enhancing the hydrogenation catalytic activity of

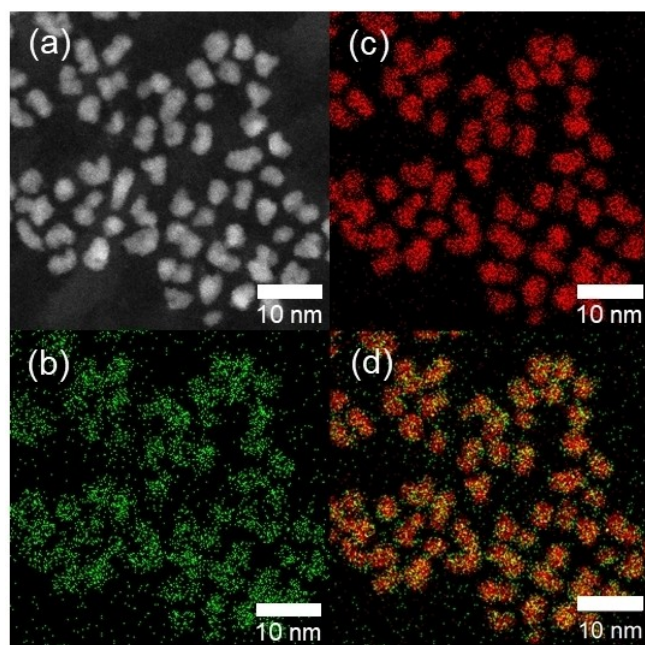


Figure 1. (a) HAADF-STEM image, (b) Mo-L, (c) Ru-L EDX maps, and (d) overlay image of $\text{Mo}_{0.2}\text{Ru}_{0.8}$.

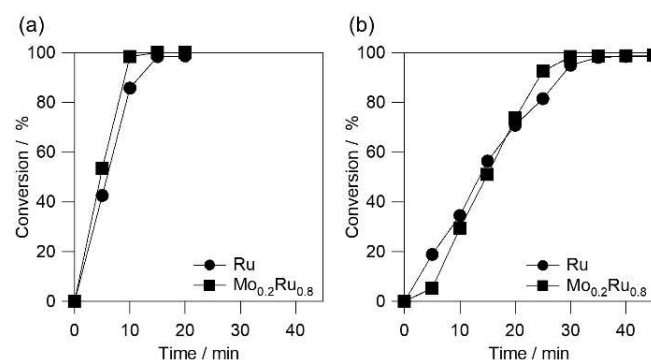


Figure 2. Time dependence of 1-octene conversion under 3.0 bar H_2 at (a) 60°C and (b) 30°C . The conversions over Ru and $\text{Mo}_{0.2}\text{Ru}_{0.8}$ are represented by circles and squares, respectively. The lines are shown as a guide for the eyes.

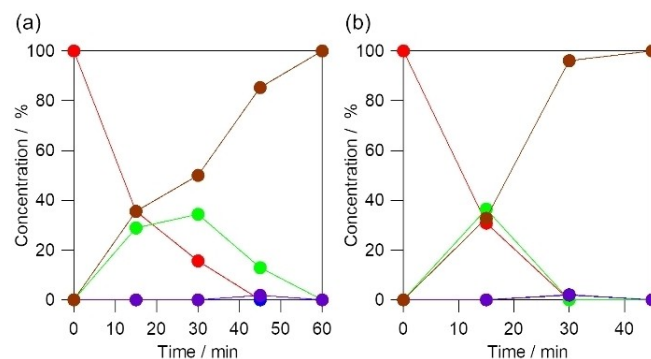


Figure 3. Time-dependent concentration of 1-octyne and the products at 60°C with (a) Ru and (b) $\text{Mo}_{0.2}\text{Ru}_{0.8}$. The concentrations of 1-octyne, 1-octene, *trans*-2-octene, *cis*-2-octene, and *n*-octane are represented by red, green, blue, purple, and brown dots, respectively. The concentrations were normalized without oligomers. The lines are shown as a guide for the eyes.

Entry	Catalyst	Temperature [°C]	H ₂ pressure [bar]	Time	Conversion [%]	<i>n</i> -Octane [%]	Oligomerization [%]
1	Ru	60	3	60 min	100	86	14
2	Mo _{0.2} Ru _{0.8}	60	3	45 min	100	86	14
3	Mo _{0.2} Ru _{0.8}	30	3	120 min	100	87	13
4	Ru	30	1	24 h	47	32	1
5	Mo _{0.2} Ru _{0.8}	30	1	24 h	100	85	15

Ru. 1-octene and *n*-octane were observed in the initial period with both NPs. This indicates that hydrogenation of 1-octene was subsequently promoted following that of 1-octyne. Therefore, both Ru and Mo_{0.2}Ru_{0.8} NPs have low selectivity for semihydrogenation. This process would be caused by the similar adsorption energies of 1-octyne and 1-octene on the NPs. Because Mo_{0.2}Ru_{0.8} NPs showed better catalytic activity, we further tested 1-octyne hydrogenation at 30 °C, which is a milder condition. As shown in Figure S10, 1-octyne and 1-octene were fully reduced within 120 min. Moreover, only Mo_{0.2}Ru_{0.8} NPs showed 100% conversion at 30 °C even under 1 bar H₂ condition, although Ru NPs showed only 47% conversion (see Table 1, entries 3 and 4). As another substrate, we selected phenylacetylene (Scheme S1 in SI) and performed their hydrogenation tests. We also confirmed the enhanced hydrogenation catalytic activity of Ru toward phenylacetylene (Table S2 in SI).

Catalytic activities are strongly affected by the electronic structure of the catalyst surface. To investigate the electronic structure of Mo_{0.2}Ru_{0.8} NPs, X-ray photoelectron spectroscopy (XPS) analysis was performed. As shown in Figure 4, Ru 3p peaks of Mo_{0.2}Ru_{0.8} NPs shifted to slightly lower energy compared with those of Ru (SI, Table S2), indicating that a charge transfer from Mo to Ru occurred. It was assumed that this electronic structure change influences the adsorption energies of substrates on solid-solution alloy NPs, resulting in the enhancement of the catalytic activity of Mo_{0.2}Ru_{0.8}. We confirmed the change of the adsorption sites by alloying through CO-DRIFTS (Figures S10–S12 in SI). This also may attribute to the enhancement of catalytic activity. In summary,

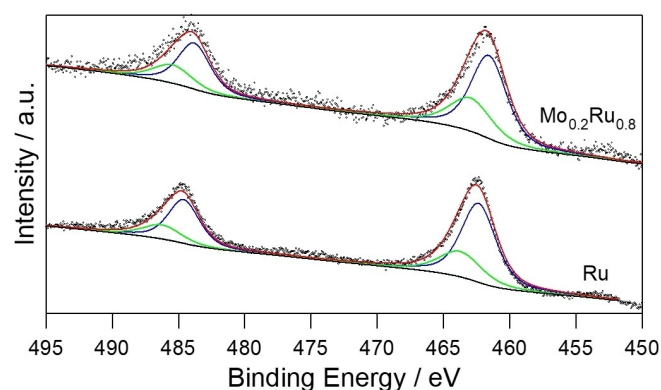


Figure 4. XPS spectra of Ru and Mo_{0.2}Ru_{0.8} NPs. The observed spectra, sum of fitting peaks, and backgrounds are represented by gray dots, red, and black solid lines, respectively. The fitting components of metallic and oxide are represented by blue and green lines, respectively.

MoRu solid-solution alloy NPs were synthesized by thermal decomposition and characterized by STEM-EDX and PXRD. Enhancement of the hydrogenation catalytic activity of Ru NPs toward 1-octene and 1-octyne by solid-solution alloying with Mo, which is an early transition metal, was observed. This study suggests that atomic-level mixing with early transition metals has the potential to improve the catalytic properties of PGM.

Acknowledgements

This work was supported by ACCEL from the Japan Science and Technology Agency (JST), Grant Number JPMJAC1501, Grant-in-Aid for Specially Promoted Research 20H05623, and JSPS KAKENHI Grant Number 19 J15102, Japan. STEM observations were performed as part of a program conducted by the Advanced Characterization Nanotechnology Platform sponsored by The Ministry of Education, Culture, Sports, Science and Technology (MEXT), Japan. The authors thank the Deutsche Forschungsgemeinschaft (DFG) for financial support of this work in the frame of the DFG-project (project no. Fi 502/32-2). Open access funding enabled and organized by Projekt DEAL.

Conflict of Interest

The authors declare no conflict of interest.

Keywords: Alloys · Hydrogenation · Molybdenum · Nanoparticles · Ruthenium

- [1] a) G. C. Bond, P. B. Wells, *J. Catal.* **1965**, *5*, 65–73; b) G. C. Bond, P. B. Wells, *J. Catal.* **1965**, *4*, 211–219; c) G. C. Bond, G. Webb, P. B. Wells, *J. Catal.* **1968**, *12*, 157–165; d) A. S. Al-Ammar, G. Webb, *J. Chem. Soc. Faraday Trans. 1* **1979**, *75*, 195–205.
- [2] a) H. Conrad, G. Ertl, E. E. Latta, *Surf. Sci.* **1974**, *41*, 435–446; b) K. Christmann, G. Ertl, T. Pignet, *Surf. Sci.* **1976**, *54*, 365–392; c) J. A. Schwarz, *Surf. Sci.* **1979**, *87*, 525–538; d) J. T. Yates, P. A. Thiel, W. H. Weinberg, *Surf. Sci.* **1979**, *84*, 427–439.
- [3] a) A. Nowicki, Y. Zhang, B. Leger, J. P. Rolland, H. Bricout, E. Monflier, A. Roucoux, *Chem. Commun.* **2006**, 296–298; b) M. Ayyün, C. T. Stoppiello, M. A. Lebedeva, E. F. Smith, M. d. C. Gimenez-Lopez, A. N. Khlobystov, T. W. Chamberlain, *J. Mater. Chem. A* **2017**, *5*, 21467–21477.
- [4] a) M. Liu, W. Yu, H. Liu, J. Zheng, *J. Colloid Interface Sci.* **1999**, *214*, 231–237; b) J. N. G. Stanley, F. Heinroth, C. C. Weber, A. F. Masters, T. Maschmeyer, *Appl. Catal. A* **2013**, *454*, 46–52.
- [5] M. Tang, S. Mao, M. Li, Z. Wei, F. Xu, H. Li, Y. Wang, *ACS Catal.* **2015**, *5*, 3100–3107.
- [6] G. Chen, S. Desinan, R. Rosei, F. Rosei, D. Ma, *Chem. Eur. J.* **2012**, *18*, 7925–7930.

- [7] H. Yang, N. Alonso-Vante, J.-M. Leger, C. Lamy, *J. Phys. Chem. B* **2004**, *108*, 1938–1947.
- [8] A. Sarkar, A. V. Murugan, A. Manthiram, *J. Mater. Chem.* **2009**, *19*, 159–165.
- [9] A. Sarkar, A. V. Murugan, A. Manthiram, *J. Phys. Chem. C* **2008**, *112*, 12037–12043.
- [10] W. Zhang, L. Wang, H. Liu, Y. Hao, H. Li, M. U. Khan, J. Zeng, *Nano Lett.* **2017**, *17*, 788–793.
- [11] S. Okazoe, K. Kusada, D. Wu, T. Yamamoto, T. Toriyama, S. Matsumura, S. Kawaguchi, Y. Kubota, H. Kitagawa, *Chem. Commun.* **2020**, *56*, 14475–14478.

Manuscript received: December 21, 2020
Revised manuscript received: February 20, 2021
Accepted manuscript online: February 22, 2021
